Synlett K. Cocq et al. Cluster

Aromatic Rings and Aromatic Rods: Nonplanar Character of an Indeno-dehydro[14]annulene

Kévin Cocq[a,b]
Nathalie Saffon-Merceron[c]
Albert Poater[d]
Valérie Maraval*[a,b]
Remi Chauvin*[a,b]

[a] CNRS, LCC (Laboratoire de Chimie de Coordination), 205 route de Narbonne, BP44099, 31077 Toulouse Cedex 4, France
valerie.maraval@lcc-toulouse.fr
chauvin@lcc-toulouse.fr
[b] Université de Toulouse, UPS, ICT-FR 2599, 31062 Toulouse Cedex 9, France
[c] Université de Toulouse, UPS, Institut de Chimie de Toulouse ICT-FR-2599, 118 Route de Narbonne, 31062 Toulouse Cedex 9, France
[d] Institut de Química Computacional i Catàlisi and Departament de Química, Universitat de Girona, Campus Montilivi, 17003 Girona, Catalonia, Spain

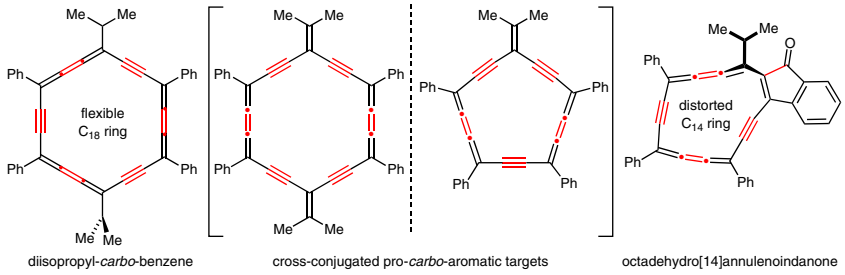

diisopropyl-*carbo*-benzene cross-conjugated pro-*carbo*-aromatic targets octadehydro[14]annulenoindanone

Received: 11.05.2016
Accepted after revision: 04.07.2016
Published online: 20.07.2016
DOI: 10.1055/s-0035-1562720; Art ID: st-2016-w0336-c

Abstract Since the concept of aromaticity has been proposed to be generalizable to acetylenic rods ('linear ring' of [2]annulene), *p*-diisopropyl-tetraphenyl-*carbo*-benzene ($C_{48}H_{34}$) and an indenone-fused isopropyl-triphenyloctadehydro[14]annulene ($C_{42}H_{26}O$) can be regarded as based on heptacyclic aromatic cores. The formation and X-ray crystal structures of both products are described. The latter has been obtained as a reductive rearrangement product of a transient isopropyl-pentaoxy[5]pericyclyne devised as a putative precursor of a *carbo*-fulvene target. A mechanism accounting for this peculiar transformation is proposed. Deviation from global planarity is measured by a 6° angle between the mean plane of the indenone bicycle and that of 13 atoms of the [14]annulenic macrocycle, forming dihedral angles with the local plane of the isopropyl-substituted sp^2 vertex of 16° and 15°, respectively. The magnetic aromaticity of the *carbo*-benzene and indeno-octadehydro[14]annulene products is evaluated by NICS calculations.

Key words alkyne, [14]annulene, aromaticity, *carbo*-benzene, indenone

1 Introduction

Beyond the equilibrium context, nonplanarity may be appraised from the standpoint of flexibility, and the larger the empty rings (fundamental circuits), the greater their flexibility.[1] This is addressed below within the context of *carbo*-mer chemistry,[2] from the *carbo*-benzene series.[2,3] While the C_6 ring of cyclohexane is nonplanar (with a chair-chair interconversion barrier through the half-chair conformation of ca. 10 kcal/mol),[4] the *carbo*-meric C_{18} ring of [6]pericyclyne (Figure 1, a) was thus shown to be 'almost flat' with quasi-isoenergetic chair, boat, and twist-boat conformations, lying less than 2 kcal/mol above the totally planar form, with interconversion barriers in the range of 1 kcal/mol and MM2-calculated strain energies below 0.2 kcal/mol.[5] These results were later confirmed and analyzed on the basis of DFT calculation results.[6] In the aromatic series, while the C_6 ring of benzene is rigidly planar, the C_{18} ring of *carbo*-benzene was also early recognized to exhibit a planar equilibrium structure of D_{6h} symmetry, albeit in a much more flexible manner allowed by a three-time weaker energetic aromaticity, defining its '*carbo*-aromatic' nature:[2c,7] this was first claimed on the basis of X-ray diffraction (XRD) analysis of the hexaphenyl derivative in the crystal state (R^i = Ph, i = 1–6, with a maximum deviation from the mean plane of merely 0.113(8) Å),[8] then confirmed by geometry optimization at the DFT level.[9]

Within the family of aromatic systems, the *carbo*-benzene core is actually more than a π-conjugated C_{18} ring: it can indeed be considered as a fused 'heptacycle' (six C2 microcycles + one C18 macrocycle) by assigning a 'generalized aromatic character' to triple or cumulenic *sp*-C–*sp*-C bonds (Figure 1, b). This is naturally achieved by extension of the [N]annulene series (N ≥ 3) to the limiting case of acetylene (N = 2). Beyond the formal issue, the relevance of this generalization is not only established within the framework of chemical (spectral) graph theory,[10] but also supported by common physicochemical features shared by classical [4n+2]annulenes and acetylene (e.g., diatropic ring current with outer magnetic deshielding effect decreasing with ring size).[2c,7] Two kinds of ideal aromatic units can therefore be distinguished: planar rings and linear rods, both kinds being condensed in the *carbo*-benzene core.

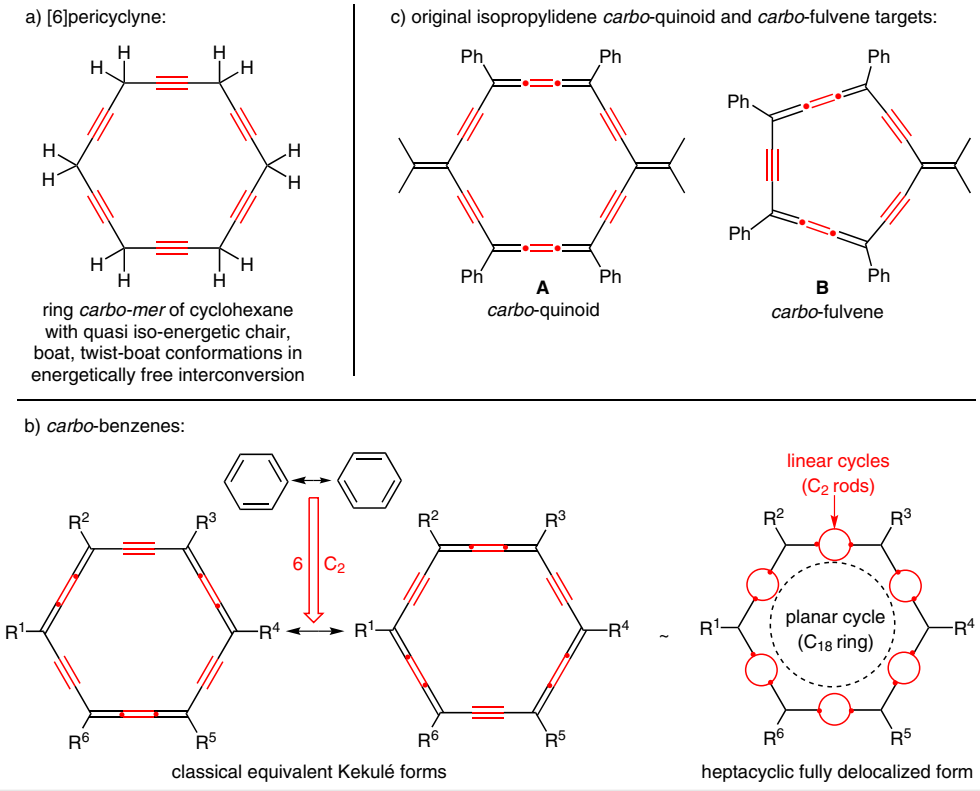

Figure 1 Typology of ring *carbo*-mers (see main text): (a) nonaromatics, (b) aromatics, (c) pro-aromatics

Most of the *carbo*-benzenes reported to date bear aromatic substituents, and the sole alkyl-substituted example, described by Ueda, Kuwatani et al., is an octupolar tris-*tert*-butyl derivative, the X-ray crystal structure of which is, however, missing. The challenge is hereafter first addressed in the quadrupolar series with two isopropyl substituents. After a recent report on difluorenylidene *carbo*-quinoids,[11] the disclosed results are spin-offs of the search for other targets, that is, the diisopropylidene *carbo*-quinoid **A** and *carbo*-fulvene **B** (Figure 1, c).[13]

2 Results and Discussion

Conditions for the formation of two novel isopropyl-substituted *carbo*-aromatics are hereafter described. Their structures are discussed with emphasis on their planar/nonplanar characters, and their local aromatic character appraised from DFT calculations of NICS.

2.1 Diisopropyltetraphenyl-*carbo*-benzene

Following the unique strategy hitherto employed for the synthesis of *carbo*-benzenes, the target **1** was envisaged by reductive aromatization of a pericyclynediol precursor **2** (Scheme 1). The formation of the C_{18} ring of **2** was envisaged through a [11+7] cyclization process from the C_{11} dinucleophile **3** and the C_7 dielectrophile **4**. The tetraynol **3** was prepared in two steps by reaction of two equivalents of the known ether-diyne **5** with methyl isobutyrate,[8] giving the tetraynol **6** in 93% yield, followed by protodesilylation with K_2CO_3/MeOH, here occurring in 91% yield. In a parallel manner, the diketone **4** was obtained by reaction of two equivalents of the dilithium salt of phenylethynylcarbinol **7** with methyl isobutyrate, giving the diynetriol **8** in 52% yield, followed by IBX-mediated oxidation, occurring in 90% yield. Incidentally, during unfruitful attempts at synthesizing the *carbo*-fulvene **B**, submitting **4** to O-mesylation–elimination conditions led to the cross-conjugated ene-di(ynone) **9** in 99% yield.[13]

The cyclization step called for optimized conditions, consisting in the treatment of the diketone **4** and tetraynol **3** in the presence of a large excess of LiHMDS. The use of such a weak reversible base indeed allows preventing the formation and precipitation of both the trianion of **3** and tetraanion of **2** (or intermediate monoadduct). After treatment with aqueous NH_4Cl, the [6]pericyclynetetraol **2** was thus isolated in 44% yield.

Ultimate treatment of **2** with the classical acidic-reducing system $SnCl_2$/HCl afforded the target *carbo*-benzene **1**, which was purified by silica gel chromatography, and iso-

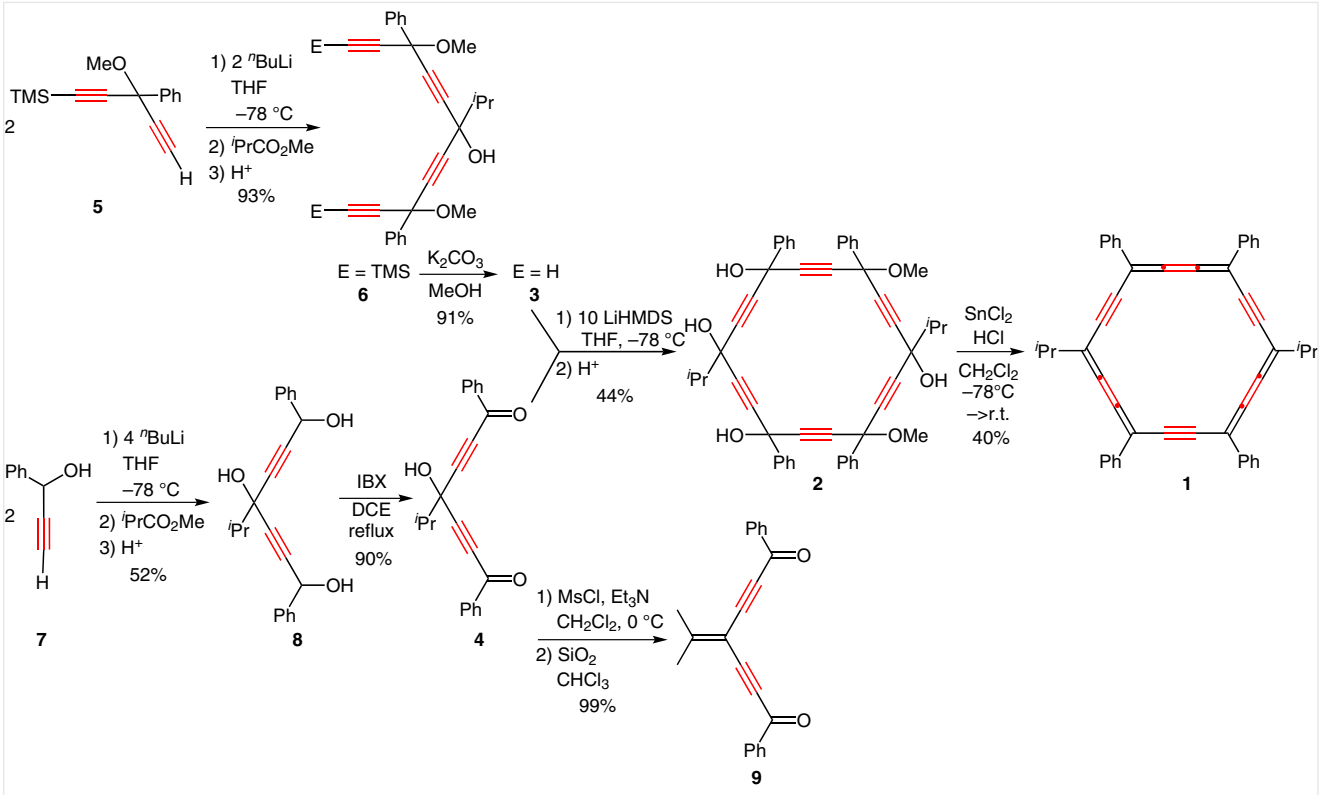

Scheme 1 Synthesis of the diisopropyltetraphenyl-*carbo*-benzene **1** from the [6]pericyclynediol **2**, obtained through a [11+7] cyclization route

lated as a dark violet solid in 40% yield. It is noteworthy that the *carbo*-quinoid **A**, an a priori possible side product,[11] was not detected.[12]

The structure was first indicated by high resolution MALDI-ToF MS spectrometry (HRMS m/z = 610.2661). The extremely poor solubility of pure **1** prevented its characterization by ^{13}C NMR spectroscopy, but tediously acquired ^{1}H NMR data are fully consistent with previous reports on *carbo*-benzenes.[2,3,14] In particular, the high magnetic aromaticity of **1** is evidenced by a strong deshielding of both the *ortho*-^{1}H nuclei of the phenyl rings (δ = 9.54 ppm, d, $^{3}J_{HH}$ = 7.7 Hz), and the ^{1}H nuclei of the ^{i}Pr substituents (δ = 5.05 ppm (sept.), 2.50 ppm (d), $^{3}J_{HH}$ = 6.9 Hz). The usually very high extinction coefficient of *carbo*-benzenic chromophores made also possible the recording of a UV-vis absorption spectrum in a chloroform solution (Figure 2), giving a further signature of the *carbo*-benzene structure (λ_{max} = 446 nm, with satellite peaks at 502, 524 and 551 nm).[14] A shoulder at λ = 435 nm is reminiscent of the one previously observed at λ = 427 nm in the absorption spectrum of the tetraphenyl-*carbo*-benzene congener with the same quadrupolar symmetry pattern without the ^{i}Pr substituents ($R^1 = R^4$ = H, $R^2 = R^3 = R^5 = R^6$ = Ph, Figure 1, b).[15]

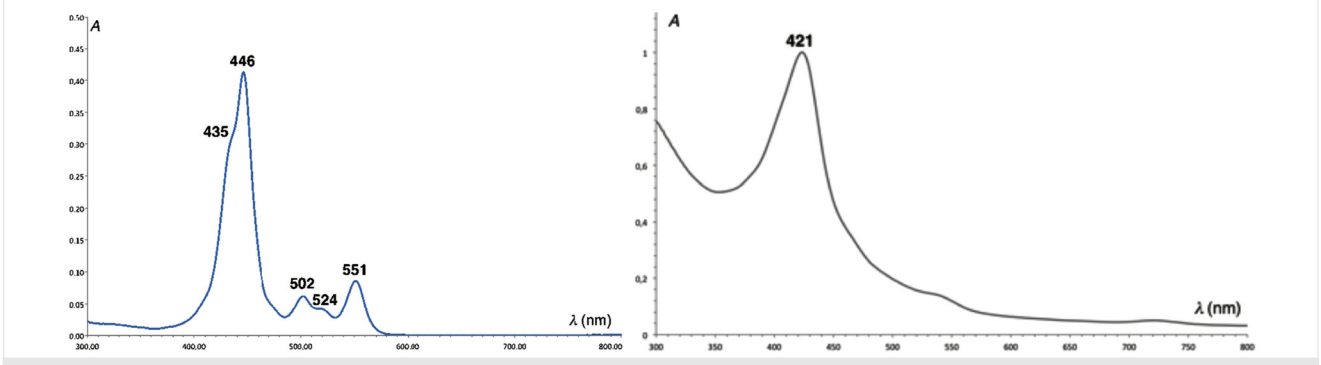

Figure 2 UV-vis absorption spectra of the *carbo*-benzene **1** in chloroform (left) and indeno-octadehydro[14]annulene **12** in toluene (right)

Single crystals, deposited upon slow evaporation of a highly diluted solution of **1** in CH_2Cl_2, were submitted to XRD analysis, allowing definite confirmation of the global structure (Figure 3).[16] Structural data are characteristic of generic *carbo*-benzenes, with average sp^2C–spC and spC–spC bond lengths of 1.38 Å and 1.23 Å, respectively, and an average angle at the C_{18} ring vertices of 119.5°. The two ^{i}Pr groups are not equivalent: with respect to the C_{18} ring mean plane, the plane of the three C atoms is either quasi-orthogonal (δ = 73.5°, allowing the proximal phenyl rings to be nearly coplanar: δ′ = 0.7°), or quasi-parallel (δ = –5.1°, inducing a larger torsional angles of the proximal phenyl rings: δ′ = 6.0°). This dissymmetry also induces a distortion of the hexagonal shape of the C_{18} ring, with an axial diameter ^{i}PrC···C^{i}Pr ≈ 7.68 Å, 5% smaller than the lateral diameters PhC···CPh ≈ 8.12 Å.

Finally, regarding the 'vibrational nonplanarity' issue in the crystal state (regardless the esd values), the maximum deviation from the mean plane of the C_{18} macrocycle is ≈ 0.04 Å (with standard deviation ≈ 0.01 Å), so quite small but greater than the maximum deviation of the more rigidly planar phenyl rings (<<0.01 Å, with a negligible standard deviation).

2.2 An Indeno-octadehydro[14]annulene

Aiming first at the *carbo*-fulvene **B**, the [5]pericyclynetriol **10** was targeted through a [8+7] cyclization process from the known C_8 triyne **11** (Scheme 2)[17] and the C_7 diketone **4** (above described, Scheme 1). The dilithium salt of **11** was thus reversibly generated in the presence of ten equivalents of LiHMDS and reacted with **4** (Scheme 2), affording a complex mixture of unidentified products, among which the target **10** could be identified by ^{1}H NMR spectroscopy but not separated. The mixture was then sequentially submitted to mesylation–elimination conditions (MsCl/Et_3N) and to a reductive treatment with $SnCl_2$ (without addition of HCl). Chromatography of the crude mixture over silica gel did not allow detection of the *carbo*-fulvene **B**, but afforded a single pure product (in minute quantities) assigned to the structure **12**,[18] as determined by XRD analysis of orange crystals deposited upon slow evaporation of a chloroform solution (Figure 4),[16] and thus isolated in a 6% yield over four steps.

The unexpected product **12** is basically an indeno[14]annulene derivative with an indenone bicycle α,β-annelated to a octadehydro[14]annulene core. The catacondensed tricyclic core thus contains two (4n+2)-aromatic fundamental π circuits, with 6 and 14 conjugated π electrons, respectively. Regarding the octadehydro[14]annulene core, XRD crystallographic data give average sp^2C–spC, spC–spC, and sp^2C–sp^2C bond lengths of 1.38 ± 0.02 Å, 1.22 ± 0.02 Å, and 1.42 ± 0.02 Å, respectively (for details, see Supporting Information). While the six bond angles at the sp^2 vertices vary from 112.5° to 133.0° (with an average of 122.5°), the eight bond angles at the *sp* vertices vary from 165.5° to 176.0° (with an average of 170.7°), showing a significant planar distortion of the C_{14} ring with respect to the VSEPR rules.[1] The macrocyclic strain is also illustrated by a short C4···14 transannular distance of 3.28 Å (sum of van der Waals radii = 3.36 Å).[19]

The C_9 indenone motif is basically planar, with a maximum deviation from the mean plane (P_{9ind}) of 0.04 Å and a standard deviation of 0.01 Å (less planar than the C_6 phenyl-

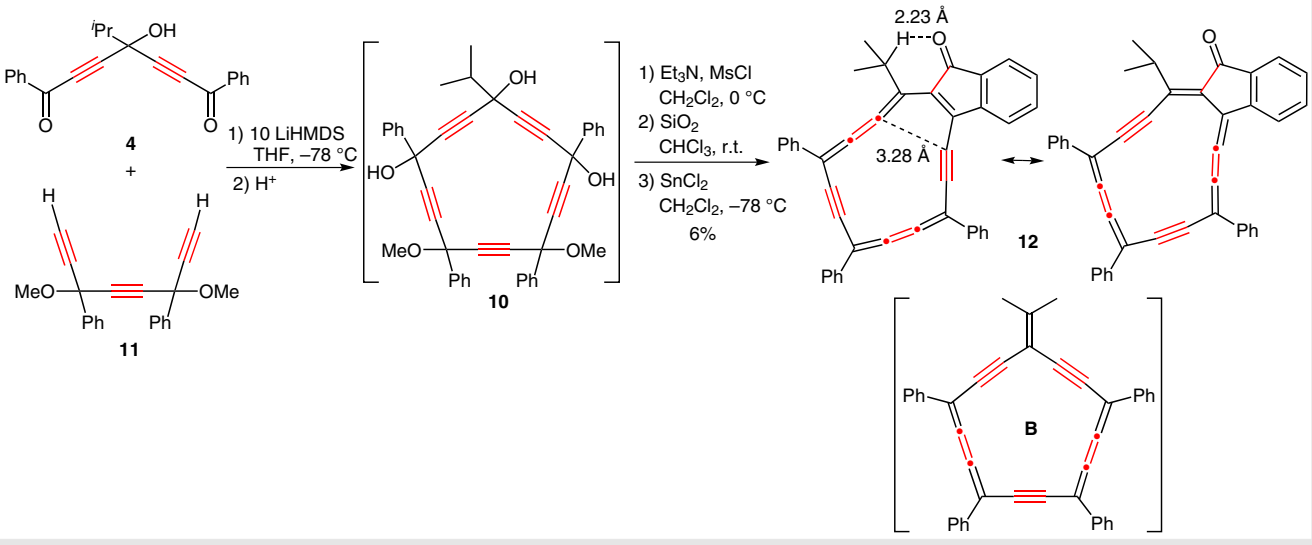

Scheme 2 In situ [8+7] generation of the [5]pericyclynetriol **10** and reductive eliminative treatment thereof, leading to the indeno-octadehydro[14]-annulene **12** (the a priori competing *carbo*-fulvene product **B** was not detected). The two internuclear distances shown on **12** correspond to crystallographic data.

ene component, with negligible maximum and standard deviations, <<0.01 Å). The dehydro[14]annulene ring is significantly puckered, especially at the level of the sp^2 vertex (C3) bearing the ^{i}Pr substituent: while the other 13 C atoms remain relatively coplanar, with a maximum deviation from the mean plane (P_{13an}) of 0.07 Å (and a standard deviation of 0.02 Å), the C3 vertex and the secondary C atom of the ^{i}Pr substituent lie 0.25 Å and 0.65 Å above this plane, respectively. This corresponds to a tilting angle of the C13–^{i}Pr bond of 15.4°. The local plane of the ^{i}Pr-substituted sp^2 vertex thus also form an angle of 15.4° with P_{13an}, and an angle of 15.7° with P_{9ind}. Finally, the global nonplanarity of the tricyclic condensed core of **12** is measured by a 6.2° dihedral angle between P_{13an}, and P_{9ind}.

The structure of **12** was further characterized by mass spectrometry (DCI/CH_4 HRMS m/z = 546.1984 [M^+]), ^{1}H NMR, and IR and UV-vis absorption spectroscopy (Figure 2, b). In particular, the C=O stretching frequency value (ν_{CO} = 1723 cm^{-1}) is slightly higher than those of 2,3-disubstituted indenones (1705 cm^{-1}),[20] and even fluorenone (1715 cm^{-1}),[21] in accordance with a relatively high aromatic character of the annelated [14]annulene ring. In the electronic spectrum, the intense absorption band at λ_{max} = 421 nm is in the range of values recorded for isolated dialkynylbutatriene motifs,[22] each Kekulé form of **12** containing one such motif. With respect to **1** (λ_{max} = 446 nm), the significantly lower λ_{max} value of **12** suggests that the involved excited states are higher in energy, and that the highly dissymmetrized C_{14} π-conjugated ring of **12** is less aromatic than the quasi-D_{6h}-symmetric C_{18} ring of *carbo*-benzenes. Using the Firefly program,[23] preliminary DFT calculations also suggest that the main UV-vis transition involves non-minimal excitations.[24]

The redox level of the carbon skeleton of **12** (ζ = 25) is just two units lower than that of **10** (ζ = 27),[25] and thus corresponds to a reduction by a single equivalent of $SnCl_2$. In spite of a very low yield, the formation of the indenone ring, a general challenge in preparative organic synthesis,[26] is here intriguing. A consistent mechanism for the transformation **10** → **12** can, however, be proposed (Scheme 3). It takes into account the specific occurrence of the isopropyl substituent of the macrocycle, making the stabilized electrophilic intermediate **I** key for an intramolecular Friedel–

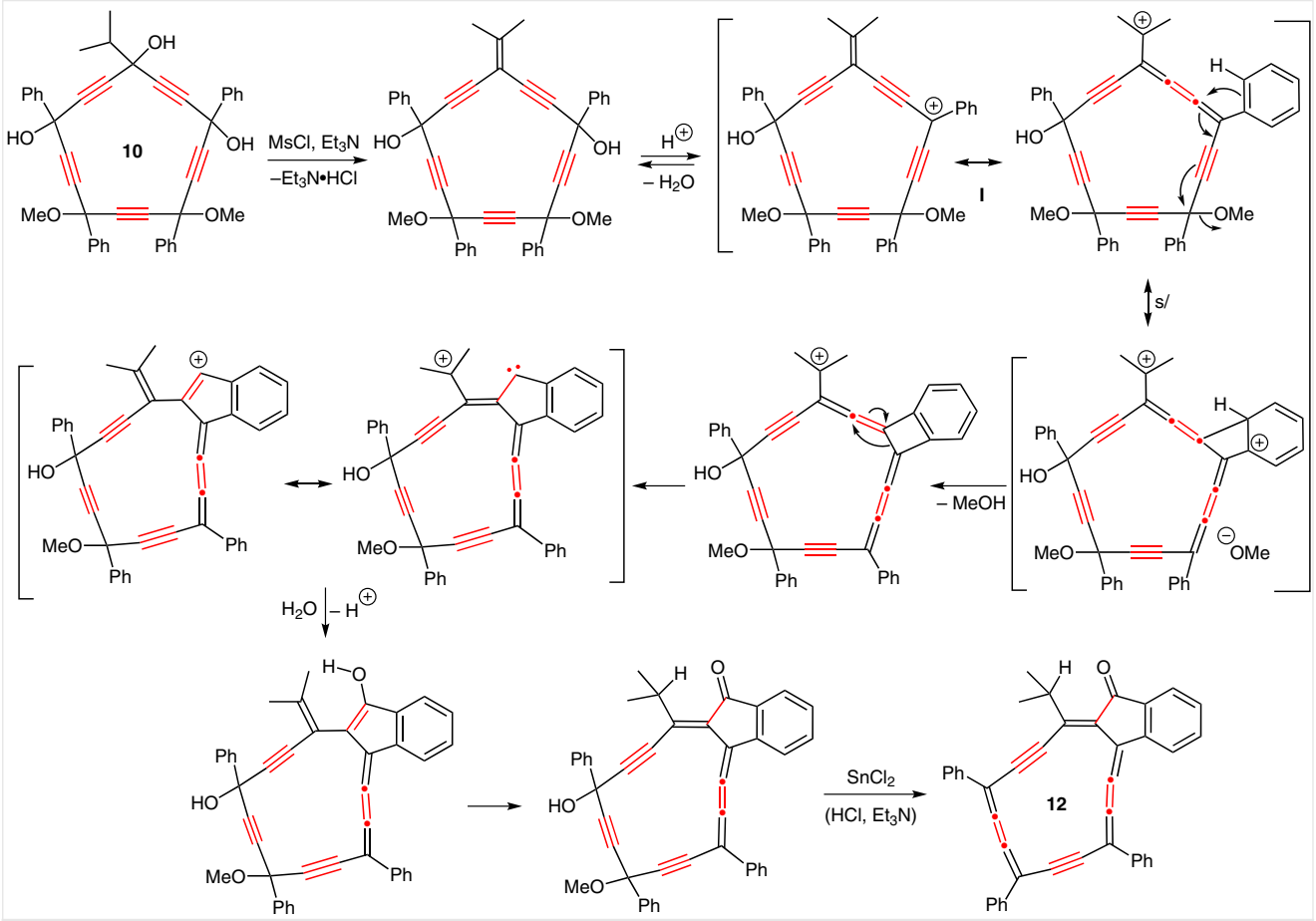

Scheme 3 Possible mechanism, allowed by the putative intermediate **I**, for the transformation of **10** to **12** under the conditions shown in Scheme 2

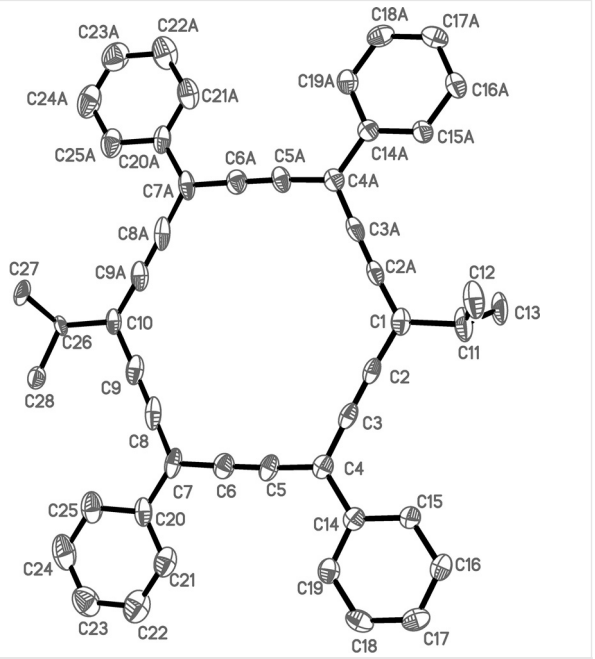

Figure 3 Molecular view of the crystallographic structure of the *carbo*-benzene **1**, with thermal ellipsoids drawn at the 50% probability level (for clarity, the H atoms are omitted). Tetragonal space group ($P\bar{4}2_1m$), with one co-crystallized CH_2Cl_2 molecule per motif of **1** (for more details, see Supporting Information).[16] Selected bond distances (Å) and bond angles (degrees): C1–C2, 1.37(1); C3–C4, 1.38(1); C4–C5, 1.40(1); C6–C7, 1.39(1); C7–C8, 1.38(1); C9–C10, 1.35(1); C10–C9A, 1.40(2); C2–C3, 1.23(1); C5–C6, 1.22(1); C8–C9, 1.23(1); C1–C11, 1.55(1); C11–C12, 1.45(2); C11–C13, 1.46(3); C10–C26, 1.52(1); C26–C27, 1.56(2); C26–C28, 1.52(5); C2A–C1–C2, 120.4(6); C3–C4–C5, 118.3(4); C6–C7–C8, 117.5(5); C9–C10–C9A, 121.6(6); C1–C2–C3, 177.1(5); C2–C3–C4, 178.8(5); C4–C5–C6, 176.6(5); C5–C6–C7, 178.7(5); C7–C8–C9, 179.1(6); C8–C9–C10, 176.8(6); C3–C4–C14–C15, –0.7; C6–C7–C20–C21, 6.0; C9–C10–26–C28, –5.1; C2–C1–C11–C13, 73.5.

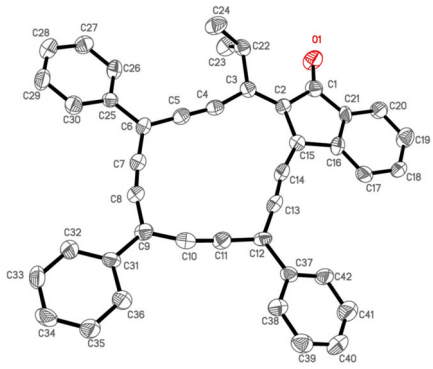

Figure 4 Molecular view of the X-ray crystallographic structure of **12**, with thermal ellipsoids drawn at the 50% probability level (for clarity, the H atoms are omitted). Monoclinic space group ($P2_1$), without any co-crystallized solvent molecule, final reliability factor ($I > 2\,\sigma(I)$): R_1 = 7.7% (for more details, see Supporting Information).[16] Selected bond distances (Å) and bond angles (degrees): O1–C1, 1.199(10); C1–C21, 1.475(11); C1–C2, 1.520(11); C2–C3, 1.393(10); C2–C15, 1.438(10); C3–C4, 1.383(11); C3–C22, 1.528(11); C4–C5, 1.237(11); C5–C6, 1.391(11); C6–C7, 1.379(12); C6–C25, 1.486(11); C7–C8, 1.214(12); C8–C9, 1.377(12); C9–C10, 1.398(11); C9–C31, 1.457(11); C10–C11, 1.201(11); C11–C12, 1.398(12); C12–C13, 1.383(12); C12–C37, 1.469(11); C13–C14, 1.240(12); C14–C15, 1.364(12); C15–C16, 1.499(10); C16–C21, 1.387(11); C22–C23, 1.523(12); C22–C24, 1.524(10); O1–C1–C21, 125.8(8); O1–C1–C2, 128.1(8); C21–C1–C2, 106.1(8); C3–C2–C15, 130.7(8); C3–C2–C1, 122.3(8); C15–C2–C1, 106.9(7); C4–C3–C2, 125.2(8); C4–C3–C22, 113.5(7); C2–C3–C22, 121.3(7); C5–C4–C3, 165.9(9); C4–C5–C6, 175.6(9); C7–C6–C5, 117.5(7); C7–C6–C25, 120.5(8); C5–C6–C25, 122.0(8); C8–C7–C6, 174.4(10); C7–C8–C9, 165.5(9); C8–C9–C10, 112.5(8); C8–C9–C31, 123.2(7); C10–C9–C31, 124.4(8); C11–C10–C9, 166.2(10); C10–C11–C12, 176.0(10); C13–C12–C11, 115.9(8); C13–C12–C37, 123.7(8); C11–C12–C37, 120.5(8); C14–C13–C12, 174.6(9); C13–C14–C15, 167.0(9); C14–C15–C2, 133.0(7); C14–C15–C16, 118.9(8); C2–C15–C16, 108.0(7); C17–C16–C15, 130.8(8); C21–C16–C15, 108.9(7); C20–C21–C16, 121.8(8); C20–C21–C1, 128.1(8); C16–C21–C1, 109.9(7); C23–C22–C24, 110.4(7); C23–C22–C3, 109.8(7); C24–C22–C3, 112.7(7).

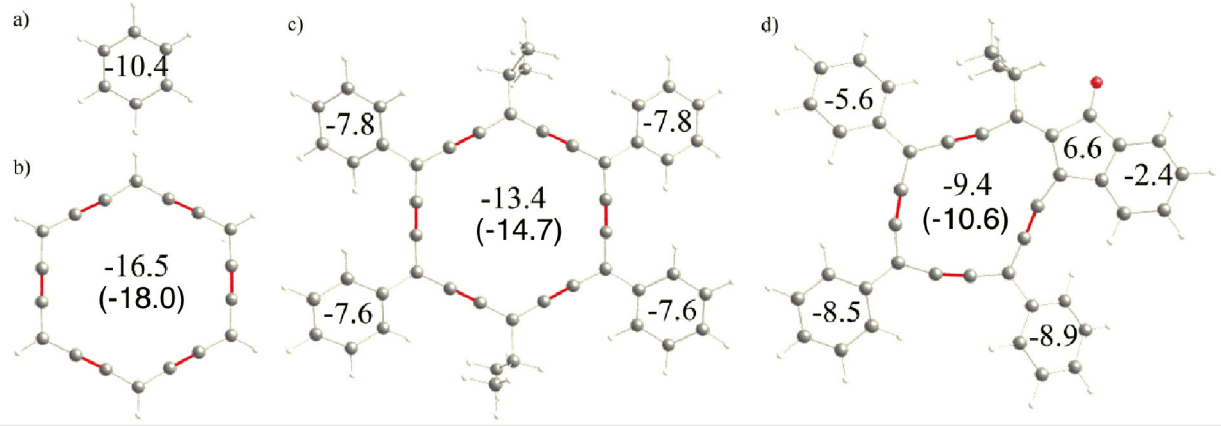

Figure 5 $NICS(1)_{out}$ values, in ppm, for benzene (a), unsubstituted *carbo*-benzene (b), diisopropyl-tetraphenyl-*carbo*-benzene **1** (c), and indeno-octadehydro[14]annulene. In parentheses, NICS(0) values for C_{18} and C_{14} rings (see more details and data in Supporting Information).

Craft process, followed by a 4 → 5 ring extension. The last but one step is actually naturally suggested by the short Me_2C–H···O=C nonbonding distance of 2.23 Å, deduced from XRD crystallographic data of **12** (Figure 5).

2.3 Magnetic aromatic Character of the Diisopropyl-*carbo*-benzene 1 and Indeno-octadehydro[14]annulene 12

Using Gaussian09,[27] at the same B3PW91/6-31G(d,p) level of theory as above (see Supporting Information),[24] local aromatic characters in **1** and **12** have been evaluated according to the magnetic criterion by calculation of nucleus-independent chemical-shift (NICS) values as proposed by Schleyer and co-workers,[28] with the gauge-including atomic orbital (GIAO) method.[29] The NICS is defined as the negative of the absolute magnetic shielding computed at specific points around the molecular system, in particular at a ring center (NICS(0) value), or 1 Å apart on the normal to the ring mean plane (NICS(1) value).[30] The smaller the NICS value (i.e., the more negative or the more diatropic the ring current), the more aromatic the ring. Whatever the ring environment, the NICS(1) values on both sides of the ring ($NICS(1)_{out}$ and $NICS(1)_{in}$) are considered to reflect the π-electron aromaticity more accurately than the NICS(0) value does.[31] Calculated NICS(1) values for all the rings, along with NICS(0) values for the 18- and 14-membered macrocycles, are collected in Figure 5, where values for nonsubstituted benzene (C_6H_6) and *carbo*-benzene ($C_{18}H_6$) are given as references (see Supporting Information for other NICS indices).[32] According to any NICS index, the magnetic aromaticity of a C_6 or C_{18} ring decreases with substitution: the NICS(1) value of the C_{18} macrocycle decreases by 3.1 ppm from the nonsubstituted *carbo*-benzene (–16.5 ppm) to the substituted derivative **1** (–13.4 ppm). This is parallel to the NICS(1) decrease by at least 2.6 ppm (and up 4.8 ppm) when going from benzene to phenyl substituents of **1** and **12**. As expected from general considerations, the magnetic aromaticity of the C_{14} ring of **12** is significantly weaker (NICS(1) = –9.4 ppm) than that of the C_{18} rings of **1** (–13.4 ppm). Finally, as expected as well, the cyclopentadienone ring of **12** appears definitely antiaromatic (NICS(1) = +6.6 ppm, positive value induced by a significantly paratropic ring current).

3 Conclusion

Around the way to *carbo*-quinoids and *carbo*-fulvenes, the *carbo*-benzene **1** and **12** address the issue of nonplanar aromaticity from a peculiar standpoint on peculiar examples. The disclosed results, however, illustrate the versatility – and unexpectedness – of the correlation between structure and reactivity in the *carbo*-aromatic series. Although 'linear is not planar' may sound quite formal, the flexibility induced by $(spC)_2$ 'aromatic rods' (acetylenic or cumulenic) in π-conjugated organic molecules is a source of dynamic or thermodynamic nonplanarity that may provide unique chromophoric, supramolecular, or other properties to alkyne-containing organic materials.

Acknowledgement

The authors thank the ANR program (ANR-11-BS07-016-01) for the doctoral fellowship of K.C. and working funds. The Centre National de la Recherche Scientifique (CNRS) is also acknowledged for half a teaching sabbatical for R.C. in 2015–2016. A.P. thanks the Spanish MINECO for a project CTQ2014-59832-JIN.

Supporting Information

Supporting information for this article is available online at http://dx.doi.org/10.1055/s-0035-1562720. Synthesis procedures and characterizations for all new compounds, structure determinations by X-ray crystallography, results of DFT calculations, and computation of various NICS indices on **1** and **12** are included.

References and Notes

(1) The larger the number of atoms prone to undergo slight strains vs. the ideal VSEPR configuration (Gillespies' valence shell electron pair repulsion model), the larger the allowed global out-of-plane deformation of the ring, the angular strain being spread out over all the endocyclic atoms.
(2) For general references on *carbo*-mers, see: (a) Chauvin, R. *Tetrahedron Lett.* **1995**, *36*, 397. (b) Maraval, V.; Chauvin, R. *Chem. Rev.* **2006**, *106*, 5317. (c) Cocq, K.; Lepetit, C.; Maraval, V.; Chauvin, R. *Chem. Soc. Rev.* **2015**, *44*, 6535.
(3) For early results on *carbo*-benzenes, see: (a) Kuwatani, Y.; Watanabe, N.; Ueda, I. *Tetrahedron Lett.* **1995**, *36*, 119. (b) Chauvin, R. *Tetrahedron Lett.* **1995**, *36*, 401.
(4) (a) Jensen, F. R.; Noyce, D. S.; Sederholm, C. H.; Berlin, A. J. *J. Am. Chem. Soc.* **1960**, *82*, 1256. (b) Anet, F. A.L.; Bourn, A. J. R. *J. Am. Chem. Soc.* **1967**, *89*, 760.
(5) (a) Scott, L. T.; DeCicco, G. J.; Hyunn, J. L.; Reinhardt, G. *J. Am. Chem. Soc.* **1985**, *107*, 6546. (b) Houk, K. N.; Scott, L. T.; Rondan, N. G.; Spelleyer, D. C.; Reinhardt, G.; Hyunn, J. L.; DeCicco, G. J.; Weiss, R.; Chen, M. H. M.; Bass, L. S.; Clardy, J.; Jorgensen, F. S.; Eaton, T. A.; Sarkozi, V.; Petit, C. M.; Ng, L.; Jordan, K. D. *J. Am. Chem. Soc.* **1985**, *107*, 6556.
(6) Lepetit, C.; Silvi, B.; Chauvin, R. *J. Phys. Chem. A* **2003**, *107*, 464.
(7) Chauvin, R.; Lepetit, C.; Maraval, V.; Leroyer, L. *Pure Appl. Chem.* **2010**, *82*, 769.
(8) Suzuki, R.; Tsukuda, H.; Watanabe, N.; Kuwatani, Y.; Ueda, I. *Tetrahedron* **1998**, *54*, 2477.
(9) (a) Godard, C.; Lepetit, C.; Chauvin, R. *Chem. Commun.* **2000**, 1833. (b) Lepetit, C.; Godard, C.; Chauvin, R. *New J. Chem.* **2001**, *25*, 572.
(10) (a) Chauvin, R.; Lepetit, C. *Phys. Chem. Chem. Phys.* **2013**, *15*, 3855. (b) Cocq, K.; Maraval, V.; Saffon-Merceron, N.; Chauvin, R. *Chem. Rec.* **2015**, *15*, 347.
(11) Cocq, K.; Maraval, V.; Saffon-Merceron, N.; Saquet, A.; Lepetit, C.; Poidevin, C.; Chauvin, R. *Angew. Chem. Int. Ed.* **2015**, *54*, 2703.

(12) The term '*carbo*-fulvene' is employed here for the first time. The actual nomenclature of **B** is: 1,4,7,10-tetraphenyl-13-(propan-2-ylidene)cyclopentadeca-1,2,3,7,8,9-hexaen-5,11,14-triyne.
(13) In tentative efforts aiming at accessing the *carbo*-quinoid **A**, conditions for a selective reaction of the ene-di(ynone) **9** with TMS-C≡C–Li could not be found. In an alternative approach, attempts at mesylation–elimination at the isopropylcarbinol vertices of the [6]periclynediol **2** also failed to produce **A**.
(14) (a) Leroyer, L.; Lepetit, C.; Rives, A.; Maraval, V.; Saffon-Merceron, N.; Kandaskalov, D.; Kieffer, D.; Chauvin, R. *Chem. Eur. J.* **2012**, *18*, 3226. (b) Baglai, I.; de Anda-Villa, M.; Barba-Barba, R. M.; Poidevin, C.; Ramos-Ortíz, G.; Maraval, V.; Lepetit, C.; Saffon-Merceron, N.; Maldonado, J.-L.; Chauvin, R. *Chem. Eur. J.* **2015**, *21*, 14186.
(15) The parent tetraphenyl-*carbo*-benzene, was, however, obtained in the presence of an undetermined impurity evidenced by ^{1}H NMR spectroscopy, see ref. 10b.
(16) CCDC 1479480 (**1**) and 1479481 (**12**) contain the supplementary crystallographic data for this paper. The data can be obtained free of charge from The Cambridge Crystallographic Data Centre via www.ccdc.cam.ac.uk/getstructures.
(17) (a) Maurette, L.; Tedeschi, C.; Sermot, E.; Soleilhavoup, M.; Hussain, F.; Donnadieu, B.; Chauvin, R. *Tetrahedron* **2004**, *60*, 1077. (b) Leroyer, L.; Zou, C.; Maraval, V.; Chauvin, R. *C. R. Chim.* **2009**, *12*, 412.
(18) The conversion of **10** to **12** proceeded in three steps.
(i) **First Step**
A solution of impure **10** (74 mg) in CH_2Cl_2 (15 mL) was treated at 0 °C with Et_3N (0.32 mL, 2.30 mmol) and mesyl chloride (0.18 mL, 2.33 mmol). The resulting mixture was stirred for 2 h at 0 °C, before dilution with CH_2Cl_2 (20 mL). After successive treatments with distilled water, sat. aq solution of $NaHCO_3$, 1 N aq solution of HCl, and extractions with CH_2Cl_2, the combined organic layers were washed with brine, dried over $MgSO_4$, and concentrated under reduced pressure without going to dryness.
(ii) **Second Step**
The concentrated solution resulting from the first step was diluted with $CHCl_3$ (20 mL) and treated at r.t. with silica (2 g). The mixture was stirred for 4 h at r.t., before filtration through Celite® and concentration under reduced pressure without going to dryness.
(iii) **Third Step**
The concentrated solution obtained from the second step was diluted with CH_2Cl_2 (20 mL) and treated at –78 °C with $SnCl_2$ (310 mg, 1.63 mmol). The resulting mixture was stirred for 20 min at –78 °C and for 2.5 h at r.t., before filtration through Celite® and silica gel and concentration under reduced pressure. Purification by silica gel chromatography (pentane–CH_2Cl_2, 8:2) afforded **12** as orange crystals (4 mg, 7.3 mmol, 6% yield from **4** or **11**).
Analytical Data for Compound 12
^{1}H NMR (400 MHz, 298 K, $CDCl_3$): δ = 1.85 (d, $^3J_{H-H}$ = 6.7 Hz, 6 H, $CH(CH_3)_2$), 5.80 (m, 1 H, $-CH(CH_3)_2$), 7.40–7.81 (m, 12 H, *m*-, *p*-C_6H_5 and -$C^{1,2,3}H$), 8.30 (d, $^3J_{H-H}$ = 7.6 Hz, 1 H, -C^4H), 8.64, 8.71, 8.78 (3 d, 3 $^3J_{H-H}$ = 7.4 Hz, 3 × 2 H, *o*-C_6H_5, without assignment). $^{13}C\{^1H\}$ NMR (100 MHz, 298K, $CDCl_3$): δ = 25.12 ($CH(CH_3)_2$), 31.49 ($CH(CH_3)_2$), 124.17, 124.28, 129.19, 129.31, 129.43, 129.68, 129.82, 129.88, 130.51, 134.43, 135.60 135.95, 137.40, 137.98, 149.33 (*o*-, *m*-, *p*-C_6H_5 and -$C^{1,2,3,4}$H, not assigned), 196.40 (>C=O). MS (DCI/CH_4): *m/z* (%) = 546.3 (100) $[M]^+$. HRMS (DCI/CH_4): *m/z* $[M]^+$ calcd for $C_{42}H_{26}O$: 546.1984; found: 546.2006. UV-vis: λ_{max} (toluene) = 421 nm. FT-IR: ν = 730 (s), 1262 (s), 1723 (s), 2924 (s) cm^{-1}.
(19) Chauvin, R. *J. Phys. Chem.* **1992**, *96*, 9194.
(20) Liebeskind, L. S.; South, M. S. *J. Org. Chem.* **1980**, *45*, 5426.
(21) Eakins, G. L.; Alford, J. S.; Tiegs, B. J.; Breyfogle, B. E.; Stearman, C. J. *J. Phys. Org. Chem.* **2011**, *24*, 1119.
(22) Maraval, V.; Leroyer, L.; Harano, A.; Barthes, C.; Saquet, A.; Duhayon, C.; Shinmyozu, T.; Chauvin, R. *Chem. Eur. J.* **2011**, *17*, 5086.
(23) (a) Granovsky, A. A. *Firefly version 8* (http://classic.chem.msu.su:gran:firefly:index.html) which is partially based on the GAMESS (US) source code. (b) Schmidt, M. W.; Baldridge, K. K.; Boatz, J. A.; Elbert, S. T.; Gordon, M. S.; Jensen, J. H.; Koseki, S.; Matsunaga, N.; Nguyen, K. A.; Su, S.; Windus, T. L.; Dupuis, M.; Montgomery, J. A. *J. Comput. Chem.* **1993**, *14*, 1347.
(24) DFT calculations at the B3PW91/6-31G(d,p) level on the crude crystallographic nuclear geometry of **12** (without re-optimization of the C–H bond lengths), give an indicative HOMO–LUMO gap of 0.090 Ha, corresponding to a one-electron excitation wavelength of 506 nm (see Supporting Information). The transition associated to the observed lower λ_{max} value (421 nm) thus likely involves excitations of higher energy, such as HOMO – 1 → LUMO or HOMO → LUMO + 1 as in the Gouterman model shown to apply to *carbo*-benzene systems (see ref. 14). The HOMO and LUMO here also involve the main π system and are spread out over both the cyclopentadienone and [14]annulene rings of **12** (see Figures in Supporting Information).
(25) The calculation of the formal 'total oxidation level' ζ of an organic molecule proceeds in two steps. First, the carbon skeleton is fully saturated (to sp^3C centers only) by hydration (addition of H_2O) of all the insaturations, and fully oxygenated by replacement of all the C–heteroatom bonds by a C–O bond if the heteroatom is more electronegative than C or by a C–H bond in the contrary case. Then ζ is equated to the total number of (single) C–O bonds.
(26) Chen, B.; Xie, X.; Lu, J.; Wang, Q.; Zhang, J.; Tang, S.; She, X.; Pan, X. *Synlett* **2006**, 259.
(27) Frisch, M. J.; Trucks, G. W.; Schlegel, H. B.; Scuseria, G. E.; Robb, M. A.; Cheeseman, J. R.; Scalmani, G.; Barone, V.; Mennucci, B.; Petersson, G. A.; Nakatsuji, H.; Caricato, M.; Li, X.; Hratchian, H. P.; Izmaylov, A. F.; Bloino, J.; Zheng, G.; Sonnenberg, J. L.; Hada, M.; Ehara, M.; Toyota, K.; Fukuda, R.; Hasegawa, J.; Ishida, M.; Nakajima, T.; Honda, Y.; Kitao, O.; Nakai, H.; Vreven, T.; Montgomery, J. A. Jr.; Peralta, J. E.; Ogliaro, F.; Bearpark, M.; Heyd, J. J.; Brothers, E.; Kudin, K. N.; Staroverov, V. N.; Kobayashi, R.; Normand, J.; Raghavachari, K.; Rendell, A.; Burant, J. C.; Iyengar, S. S.; Tomasi, J.; Cossi, M.; Rega, N.; Millam, N. J.; Klene, M.; Knox, J. E.; Cross, J. B.; Bakken, V.; Adamo, C.; Jaramillo, J.; Gomperts, R.; Stratmann, R. E.; Yazyev, O.; Austin, A. J.; Cammi, R.; Pomelli, C.; Ochterski, J. W.; Martin, R. L.; Morokuma, K.; Zakrzewski, V. G.; Voth, G. A.; Salvador, P.; Dannenberg, J. J.; Dapprich, S.; Daniels, A. D.; Farkas, Ö.; Foresman, J. B.; Ortiz, J. V.; Cioslowski, J.; Fox, D. J. *Gaussian 09, Revision A.01*; Gaussian, Inc: Wallingford CT, **2009**.
(28) Schleyer, P. v. R.; Maerker, C.; Dransfeld, A.; Jiao, H. J.; Hommes, J. R. V. *J. Am. Chem. Soc.* **1996**, *118*, 6317.
(29) Wolinski, K.; Hinton, J. F.; Pulay, P. *J. Am. Chem. Soc.* **1990**, *112*, 8251.
(30) Poater, J.; Duran, M.; Solà, M.; Silvi, B. *Chem. Rev.* **2005**, *105*, 3911.
(31) Corminboeuf, C.; Heine, T.; Seifert, G.; Schleyer, P. v. R.; Weber, J. *Phys. Chem. Chem. Phys.* **2004**, *6*, 273.
(32) Turias, F.; Poater, J.; Chauvin, R.; Poater, A. *Struct. Chem.* **2016**, *27*, 240.